

NPS ARCHIVE
1969
VAN DUZER, R.

FINITE DEFLECTIONS OF RATE
INSENSITIVE PLATES AND BEAMS
SUBJECTED TO A DYNAMIC IMPULSE

LT. ROGER ELLIOTT VAN DUZER, USN

Thesis
V163

LIBRARY
NAVAL POSTGRADUATE SCHOOL
MONTEREY, CALIF. 93940

DUDLEY KNOX LIBRARY
NAVAL POSTGRADUATE SCHOOL
MONTEREY, CA 93943-5101

FINITE DEFLECTIONS OF RATE
INSENSITIVE PLATES AND BEAMS SUBJECTED
TO A DYNAMIC IMPULSE

by

Roger Elliott Van Duzer
Lieutenant, United States Navy
B.S., United States Naval Academy
(1964)

SUBMITTED IN PARTIAL FULFILLMENT
OF THE REQUIREMENTS FOR THE
DEGREE OF MASTER OF SCIENCE

IN NAVAL ARCHITECTURE AND
MARINE ENGINEERING
AND THE PROFESSIONAL DEGREE
NAVAL ENGINEER
at the
MASSACHUSETTS INSTITUTE OF
TECHNOLOGY
June, 1969

NRS ARCHIVE

1962

~~716~~
~~X16~~

VANDUZER, R.

FINITE DEFLECTIONS OF RATE INSENSITIVE PLATES
AND BEAMS SUBJECTED TO A DYNAMIC IMPULSE

by

Roger Elliott Van Duzer

Submitted in partial fulfillment of the requirements of
the requirements for the degree of Master of Science in
Naval Architecture and Marine Engineering and the profes-
sional degree Naval Engineer.

ABSTRACT

Presented herein are the results from a series of experiments to determine the permanent deformations of straight beams and rectangular plates with two edges clamped loaded by a uniform dynamic impulse. The specimens were made of 6061-T6 aluminum which is considered representative of rate-insensitive, non-strain-hardening metals. The impulse was provided by a sheet explosive. It was shown that the plate response may be described by an existing beam theory for rigid-plastic behavior which includes finite-deflections.

Thesis Supervisor: Norman Jones
Title: Assistant Professor of Naval Architecture
and Marine Engineering

TABLE OF CONTENTS

| | |
|-----------------------------------------|----|
| Abstract | 2 |
| Table of Contents | 3 |
| List of Tables | 4 |
| List of Figures | 5 |
| Introduction | 6 |
| Experimental Procedure | 9 |
| Results | 22 |
| Discussion of Results | 39 |
| Conclusions | 45 |
| References | 46 |
| Appendices | |
| Appendix A: Experimental Recommendation | 48 |
| Appendix B: Calculation of V | 49 |
| Appendix C: Tensile Test Results | 52 |
| Appendix D: Strain Gage Results | 57 |
| Appendix E: Datasheet Specifications | 60 |

LIST OF TABLES

4

| | | |
|---------------------------------------------|--|----|
| Table 1 | | |
| Chemical Analysis and Mechanical Properties | | |
| of 6061-T6 Aluminum | | 18 |
| Table 2 | | |
| Notation | | 19 |
| Table 3 | | |
| Deflections and Dynamic Parameters | | 23 |
| Table 4 | | |
| Test Description | | 25 |

LIST OF FIGURES

| | |
|------------------------------------------------------------|----|
| Figure 1 - Experimental Apparatus | 15 |
| Figure 2 - Details of Head | 16 |
| Figure 3 - Specimens | 17 |
| Figure 4 - Specimen Reference Coordinates | 21 |
| Figure 5 - W vs. X and Y for Plate No. 19 | 27 |
| Figure 6 - W vs. X and Y for Plate No. 2 | 28 |
| Figure 7 - W vs. X and Y for Plate No. 2 | 29 |
| Figure 8 - W vs. X and Y for Plate No. 13 | 30 |
| Figure 9 - W vs. X and Y for Beam No. 11 | 31 |
| Figure 10- W vs. X and Y for Beam No. 7 | 32 |
| Figure 11- W_M/H and W_O/H vs. V for $H = 0.122$ inch. | 33 |
| Figure 12- W_M/H and W_O/H vs. V for $H = 0.189$ inch. | 34 |
| Figure 13- W_M/H and W_O/H vs. V for $H = 0.246$ inch. | 35 |
| Figure 14- W_M/H vs. V | 36 |
| Figure 15- W_M/H vs. λ | 37 |
| Figure 16- W_M/H vs. λ for small λ | 38 |
| Figure 17- Stress vs. Strain for Sample No. 7 | 56 |
| Figure 18- Strain vs. Time for Beam No. 9 | 59 |

INTRODUCTION

The dynamic behavior of structures is of increasing concern to the engineer. Few designers intend to have structures experience such extremes as pressure due to explosions or significant impact as with colliding vehicles, but obviously there are many design situations in which dynamic loading must be considered. Alternatively many loads are of such high pressure to duration ratio that they may be viewed as dynamic impulses.

The study of plasticity is comparatively recent. Most engineers now employ the elastic-plastic and rigid-plastic analysis with associated limit theorems which stem from the early 1950's. Initial work on dynamic plasticity was concerned with cantilever beams subjected to impacting masses. Parkes (1) in 1955 did a series of tests on mild steel beams for which he found deformations considerably less than those predicted by rigid plastic analysis. He decided that strain-rate sensitivity accounted for most of this discrepancy. Seiler, Cotter, and Symonds (2) in 1956 postulated that a high ratio of initial kinetic energy to an upper bound of elastic strain energy was required for good results with rigid-plastic theory. In 1962, Bodner and Symonds (3) reinvestigated the earlier work of Parkes on cantilever beams and decided that strain-rate sensitivity was important. Ting (4) later substantiated this theory and observed that

geometry changes could be important for large deformations.

In 1958, Symonds and Mentel (5) examined the impulsive loading of strain beams with axial constraints and utilized rigid-plastic theory to show that the permanent deformations would be less than those predicted by a simple bending solution. Humphrey's (6) test on steel beams supported this view. The results of these tests indicated that simple theory was valid for deformations less than the beam thickness. Bodner (7) discussed a stress, strain-rate sensitivity relation postulated by Cowper and Symonds (8) and noted that those materials with sharply defined yield points were generally rate sensitive. Perrone (9) proposed a simple method and tried to justify use of a dynamic yield stress with rigid-plastic solutions. Florence and Firth (10) did experiments on pinned-end beams and improved the rigid-plastic theory by including strain-rate effects.

Jones (11) presented a method in 1967 to estimate the combined influence of strain-hardening and strain-rate sensitivity on rigid-plastic beams loaded dynamically. He suggested that both effects could be ignored for physically large beams which have a high length to thickness ratio. In 1968, Jones (12) proposed a solution for the permanent deformation of annular plates with emphasis on finite-deflections. In 1969, he complied results of beam tests and determined that finite-deflections were dominate and that strain-rate sensitivity could be disregarded in a

When permanent deformations are considered, simple bending moment theories are not always adequate. The material certainly has increased capacity to dissipate energy more efficiently through membrane forces, i.e. finite deflections. The relative importance of strain-rate sensitivity and strain-hardening is not clearly understood. There is a shortage of experimental data with which the theory may be compared. The author presents the results of tests on a series of 6061-T6 aluminum rectangular plates with two edges clamped to further research in this field. It is believed that plates are a logical extension of the study of beams. It is of interest to determine whether or not existing beam theory for permanent deformations may be extended to plates.

EXPERIMENTAL PROCEDURE

An extensive series of tests were conducted on various aluminum plates and beams of rectangular cross-sections with two ends clamped and two edges free utilizing the apparatus shown in Figures 1 and 2. Typical specimen shapes and dimensions are shown in Figure 3.

6061-T6 aluminum was chosen as a representative commercial aluminum commonly utilized and for which various strain-rate parameters had been previously determined (8, 9). Mechanical and physical properties in Table 1 were determined by testing samples from the sheets from which the test specimens were machined. The nominal thickness of the specimens chosen for testing after a mild surface polish were .089 in., .122 in., .189 in., and 0.246 in. Thickness and width readings were taken at numerous geometrically spaced points on the sample and then averaged. Variations in thickness of any plate were less than $\pm .00025$ inches while variations in width were less than $\pm .0015$ inches. All test specimens were 5.046 inches in length between the clamped edges. Most specimens were machined to approximately 3 inches in width. In an effort to discern a transition from beam to plate phenomena, a series of samples 1 in., 2 in., and 5 in. in width were tested for the thickest plate used. All test specimens were machined so that the free edges were away from regions of the received

material which showed edge effects due to the manufacturers processing techniques. Figures 7a through 7e (17) notes the location of each specimen within the original sheets received. The surfaces of the specimens were polished with fine silicon carbide paper to remove minor marks.

The head in which the specimens were clamped was welded to a backing plate to insure no axial motion of the heads. Excessive slippage of the clamped portion of the specimens was observed in an early test. There was visible necking of material between the bolts. This was reduced to an acceptable level by putting serrations in the heads and utilizing high strength bolts. Further improvements are suggested in Appendix A.

Detasheet D, a flexible sheet explosive composed of PETN and an elastomeric binder was used to provide the dynamic impulse. The explosive was received in sheets of 0.01 and 0.015 inches in thickness. The thicknesses were laminated and in certain tests perforated to achieve a range of impulsive loading. Supersonic detonation velocity is required and midspan detonation is recommended to approximate uniform initial velocity distribution along a beam. The higher the ratio of detonation velocity to the bending wave speed of the specimens the better the approximations to a uniformly distributed impulse (14). The bending wave speed for 6061-T6 is about 18,580 fps while the detonation velocity of the explosive is listed

by the manufacture as 23,000 fps.

The explosive was cut to the same dimensions as the aluminum specimens between the clamps. It was then mounted on a piece of protective material to prevent spalling of the aluminum and pitting of the plate surface. Rubber cement was sufficient as an adhesive. Electric detonators commonly known as No. 6 blasting caps ignited an explosive leader which was roughly 15 inches in length, 1/8 inch in width, and 0.015 inch in thickness. This leader detonated the test explosive at its midpoint. The leader had to be firmly pressed into the sheet explosive to insure detonation. Use of the leader allowed the detonator to be shielded.

Originally, 1/8 inch thick neoprene was used adjacent to the test specimens as in Humphrey's test (6) to prevent spalling. Many of the thin 0.089 and 0.122 inch plates sheared at the clamped edges with only 10 or 15 mils of explosive for loading. Roughly, the force of the explosion varies as the weight of explosive to the 1/3 power but inversely to the stand-off distance. To diverse the blast impulse and permit a wider range of testing a low density packing foam of 1/2 inch thickness was used for a backing material. Paper was glued between the specimen and foam and between the foam and explosive. This permitted easier handling of the explosive and provided added protection against spalling. It was observed that the foam and paper ,

disintegrated during the blast. When neoprene was used as a backing, it was found intact but blown off the plate. Thus, there was questions as to how it effected the energy balance, in particular, whether or not its mass should be included with that of the specimen between the clamps in any momentum balance.

The ballistic pendulum is an ideal device for this type of experiment. Such exotic techniques as high speed cameras may be preferred if funds are available. The blast chamber in which the tests were conducted allowed an adequate suspension height. The pendulum was made from a steel I beam and supported on spring steel wire of .02 inch diameter. The wires were angled slightly in an end on view to avoid side sway. Before each test, lead ballast weights were added to the pendulum and the wire lengths were adjusted to balance the pendulum.

The length of swing of the pendulum was recorded on a heat-sensitive paper mounted on an adjustable track. Before each test, the track was set to conform with the arc of the pendulum for its measured suspension length. The paper was marked by a tungsten wire suspended beneath the pendulum and traveling with light contact along the paper. External batteries provided power through fine leads to the tungsten wire. Tests were conducted to determine what losses in the energy balance might occur due to drag of the pendulum as it swung. These losses

were so minimal that they were not considered (15).

For each specimen tested, the following data was necessary: the thickness of explosive; the weight of the plate tested; the height of the pendulum from the floor; the weight of the test plate and added ballast; the length of swing of the pendulum; the deflections at noted points on the specimen.

Upon completion of the test, the specimens were examined for excessive slip at the clamps. Measurements of the deflection was made at various points on the specimens with a dial gage on a machined flat table.

A sample calculation of the impulse velocity, V , is presented in Appendix B. Basically, the blast loading was treated as a rectangular pressure pulse in which the pressure approaches infinite magnitude and the duration of loading goes to zero time. This is considered an impulse, the product of the mass per unit area and a velocity, V . This approach is generally accepted if the peak pressure is five to ten times greater than the static collapse pressure. The potential energy of the pendulum at its maximum swing is balanced against the initial inertial energy of the system which may then be used to determine the impulse of the mass of the specimen between the clamps.

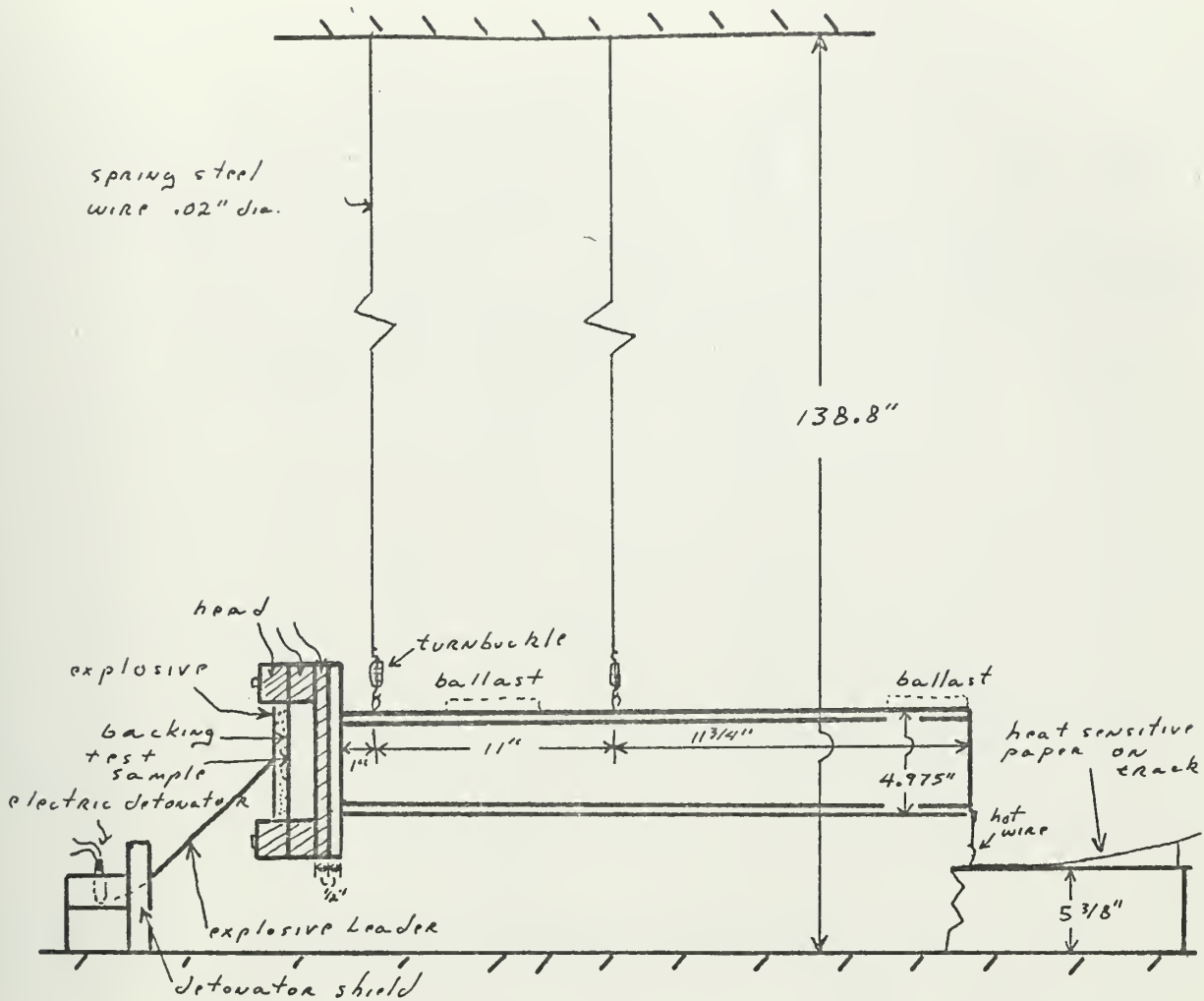
Concurrent with the main program of experimentation tests involving strain gages were conducted in an attempt to find initial strain rates of the specimens. This is

discussed in detail in Appendix D.

14

FIGURE |
EXPERIMENTAL APPARATUS

15



Pendulum weight without ballast - 20596.9 gms

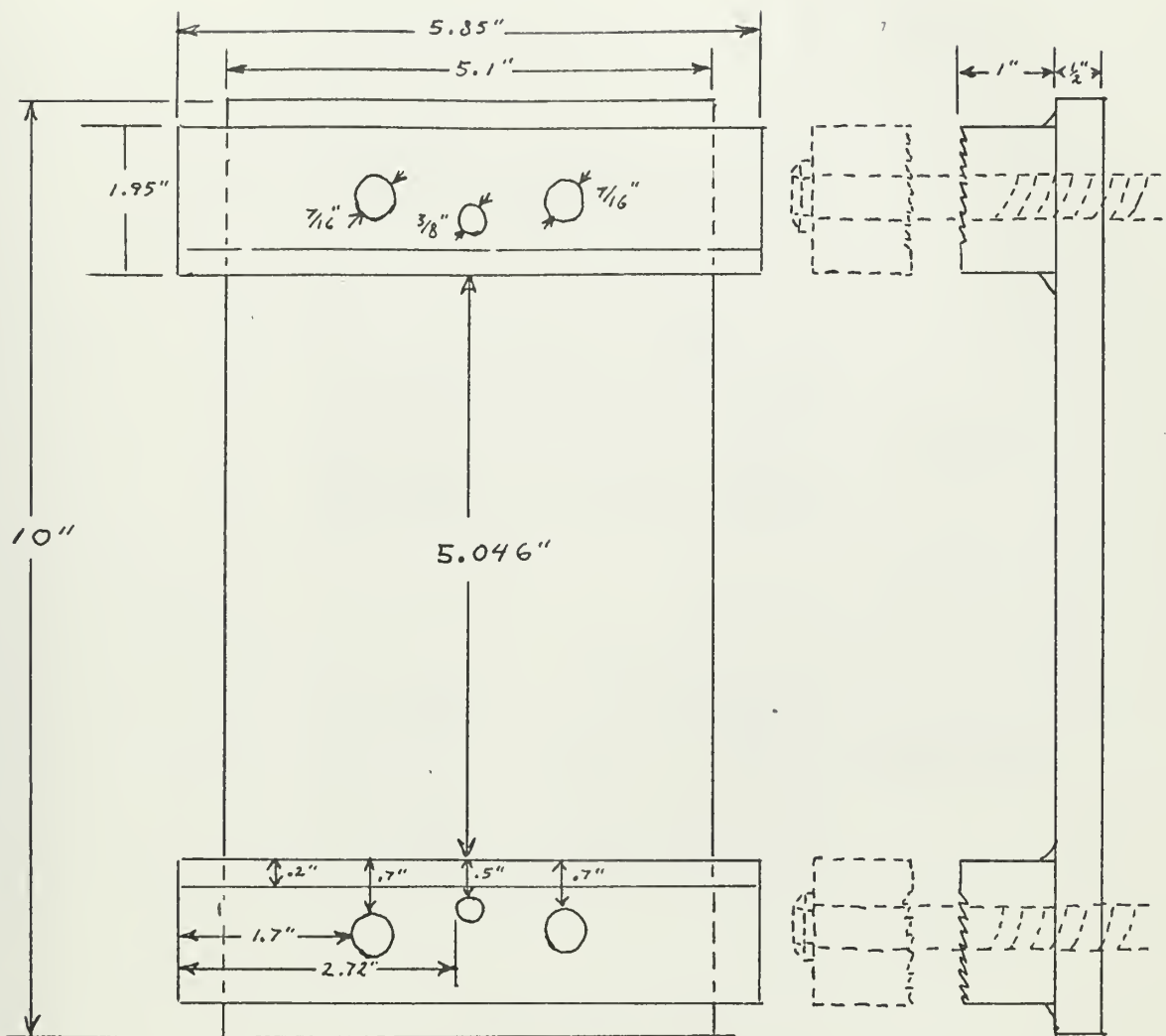
Weight of head - 8300 gms.

Weight of bolts for head - 535 gms.

FIGURE 2

Details of Head

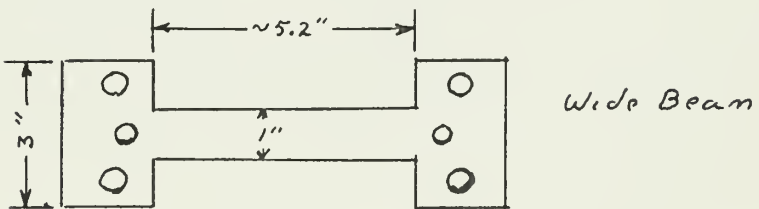
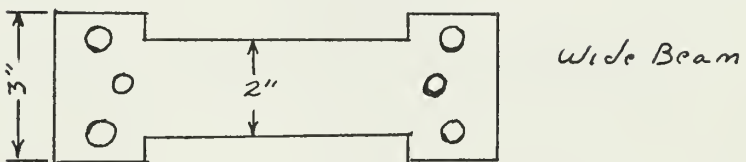
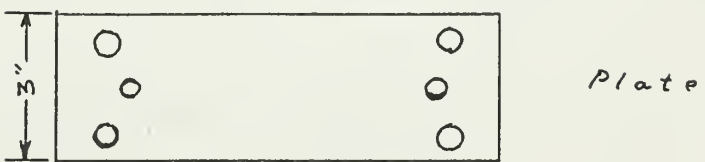
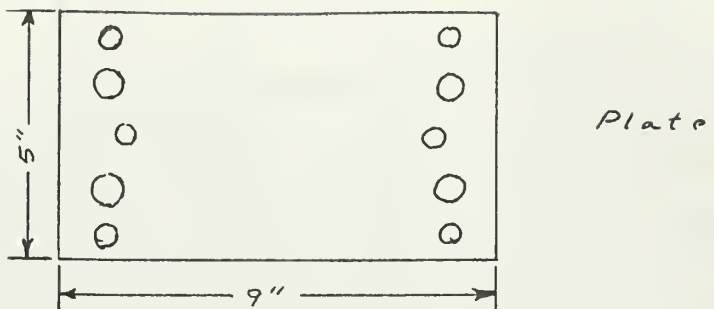
16



not to scale

FIGURE 3
Specimens

17



PLAN VIEW

TABLE 1

CHEMICAL ANALYSIS AND MECHANIC PROPERTIES
OF 6061-T6 ALUMINUM

CHEMICAL PROPERTIES

| Sample | Thickness | % Si | % Cu | % Mg | % Cr |
|--------|-----------|------|------|------|------|
| 11 | .122 in. | .65 | .20 | .85 | .26 |
| 11 | .189 in. | .61 | .21 | .83 | .21 |
| 13 | .089 in. | .57 | .24 | .89 | .23 |
| 0 | .246 in. | .60 | .24 | 1.04 | .17 |

MECHANICAL PROPERTIES
(Details in Appendix C)

Average Yield Stress $\sigma_0 = 41,212$ psi

Average Elastic Modulus $E = 10.49 \times 10^6$ psi

Average Ultimate Stress $\sigma_{ULT} = 45,660$ psi

Average Modulus of Plastic Region $E_2 = 9.78 \times 10^4$ psi

Density = .098799 lb./in.³

TABLE 2

NOTATION

| | |
|------------|---------------------------------------------------------------------------------------|
| D | strain rate sensitivity coefficient |
| E | modulus of elasticity |
| B | width of plate or beam |
| H | thickness of plate or beam |
| L | semi length of plate or beam |
| M_o | $\sigma_o H^2 / 4$ |
| V | initial velocity of beam |
| p | strain rate sensitivity coefficient |
| x | distance defined in Figure 4 |
| y | distance defined in Figure 4 |
| w_M | maximum permanent transverse displacement along $y = 0$ |
| w_o | maximum permanent transverse displacement at a location other than $y = 0$ |
| r | ratio of slopes of elastic and plastic portion of stress-strain curve |
| μ | mass per unit area of plate or beam |
| σ_o | yield stress in simple tension |
| θ | rotation in degrees of clamped portion of specimen after test as shown in Figure 4 |
| λ | $\frac{\mu V^2 L^2}{M_o H}$ |
| v | $E/\nu \sigma_o$ |
| γ | $\nu H^2 / L^2$ |

$$\alpha \quad \left(\frac{2VH}{DL^2} \right)^{1/P}$$

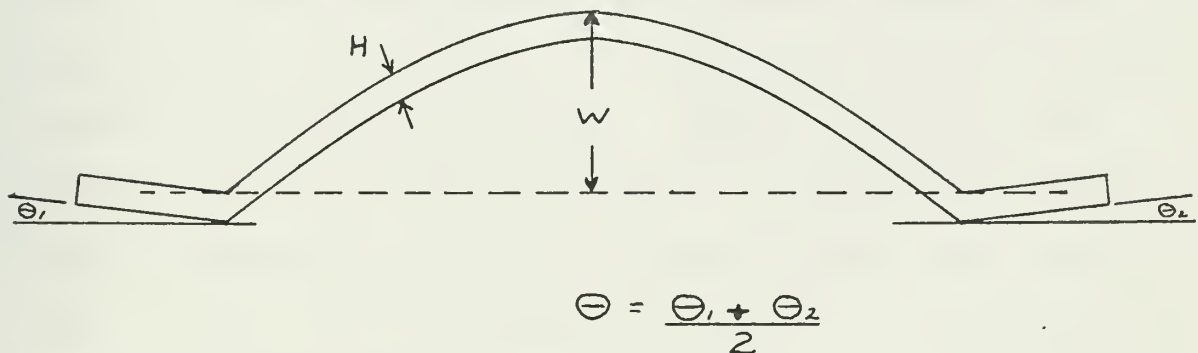
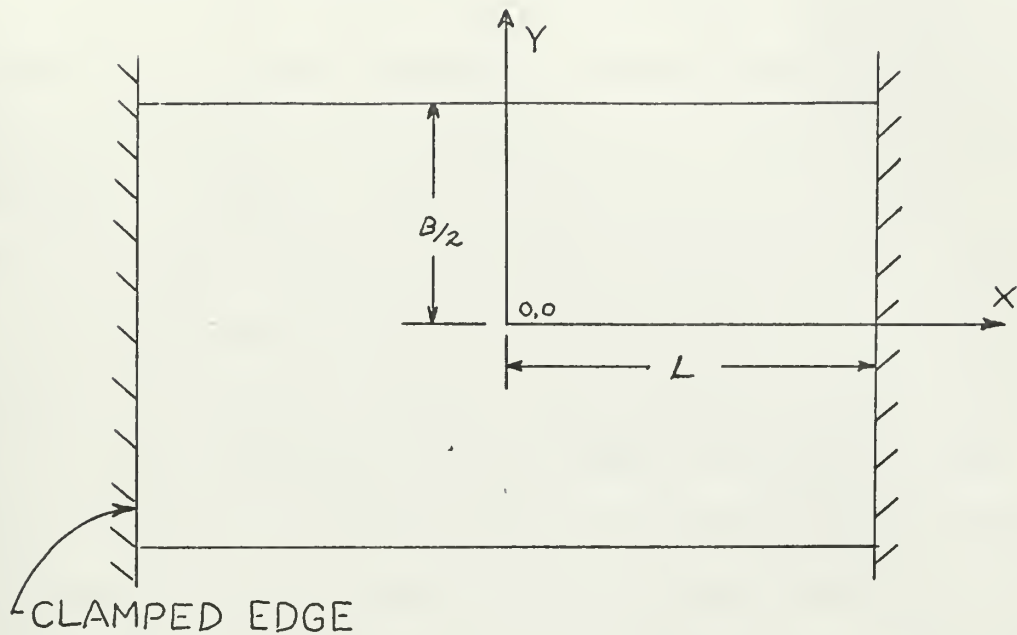
δ maximum displacement of ballistic pendulum measured from its initial position

ϵ strain

\cdot $\partial/\partial t$

FIGURE 4
SPECIMEN REFERENCE COORDINATES

21



RESULTS

The tables and figures which follow are discussed in detail in the next section. Rather than footnote a few explanatory remarks are presented now. Under "Explosive thickness" in Table 4 are entries of the form xx per. The "per" means that the explosive was perforated. Holes of 1/8 inch diameter were cut in the explosive at spaced intervals to further decrease the pressure loading. The N or F in the "Backing" column stands for neoprene and foam and refers to the attenuator used between the specimen and explosive as explained in the previous section. The terms in the "Slippage" column are qualitative. "Necking" means flow was visible in the clamped portion when the specimen was removed. "Visible" means that although necking did not occur, there was a clearly defined line which showed that the edge $X = L$ had moved slightly inwards towards the center of the beam. "Minor" signifies that slippage probably occurred but was not readily discernable. For the calculation of α , $p = 4$ and $D = 6500$ l/sec. were used (8,9). For the calculation of v , $r = 107.29$ was determined from tensile tests.

TABLE 3

| Sample | $\frac{H}{avg.}$ inch | $\frac{B}{avg.}$ inch | DEFLECTIONS AND DYNAMIC PARAMETERS | | | | |
|--------|--------------------------|--------------------------|------------------------------------|-----------------|-------------|-----------|----------|
| | | | $\frac{W_M}{H}$ | $\frac{W_O}{H}$ | V ft/sec | λ | α |
| 6 | 0.089 | 3.03 | 6.3082 | 6.6629 | 271.92 | 212.349 | 0.185 |
| 4 | 0.089 | 3.021 | 6.764 | 5.1124 | 259.35 | 193.355 | 0.183 |
| 5 | 0.089 | 3.025 | 6.7472 | 7.2191 | 264.78 | 201.536 | 0.183 |
| 2 | 0.122 | 3.021 | 3.582 | 3.836 | 252.71 | 97.69 | 0.196 |
| 3 | 0.1223 | 3.0287 | 3.115 | 3.328 | 205.41 | 64.23 | 0.187 |
| 5 | 0.1225 | 3.026 | 5.796 | 5.861 | 355.06 | 191.29 | 0.214 |
| 10 | 0.122 | 3.0263 | 3.269 | 3.531 | 212.09 | 68.26 | 0.188 |
| 20 | 0.123 | 3.019 | 3.951 | 4.163 | 243.38 | 89.88 | 0.195 |
| 21 | 0.1225 | 3.02 | 3.447 | 3.609 | 216.49 | 71.12 | 0.189 |
| 19 | 0.1225 | 3.021 | 3.728 | 3.92 | 240.68 | 87.89 | 0.194 |
| 5 | 0.189 | 3.025 | 1.191 | 1.370 | 173.92 | 19.28 | 0.199 |
| 10 | 0.189 | 3.001 | 1.791 | 1.979 | 173.04 | 19.09 | 0.199 |
| 3 | 0.188 | 3.013 | 2.937 | 3.177 | 307.21 | 60.80 | 0.229 |
| 7 | 0.189 | 3.019 | 2.706 | 2.944 | 244.41 | 38.08 | 0.217 |

Table 3 contd.

| Sample | $\frac{W_M}{H}$ | $\frac{W_O}{H}$ | V ft/sec | λ | α | γ |
|--------|-----------------|-----------------|-------------|-----------|----------|----------|
| | avg. inch | avg. inch | | | | |
| 2 | .1877 | 3.0207 | 1.891 | 2.073 | 198.16 | 25.38 |
| 9 | .189 | 2.9673 | 1.468 | | 165.22 | 17.40 |
| 1 | .1895 | 3.009 | 1.908 | 1.982 | 208.12 | 27.46 |
| 5 | .246 | 3.025 | 1.061 | 1.122 | 179.16 | 12.08 |
| 3 | .246 | 3.028 | 0.695 | 0.768 | 129.56 | 6.32 |
| 1 | .246 | 3.0253 | 0.979 | 1.028 | 162.87 | 9.96 |
| 6 | .246 | 3.023 | 1.563 | 1.689 | 231.92 | 20.24 |
| 2 | .246 | 3.0237 | 1.963 | 2.065 | 283.57 | 30.3 |
| 8 | .246 | 1.0253 | 0.474 | | 109.98 | 4.55 |
| 7 | .246 | 1.018 | 0.760 | | 148.24 | 8.27 |
| 9 | .246 | 1.0283 | 1.087 | | 193.58 | 14.10 |
| 10 | .246 | 2.011 | 0.618 | | 121.27 | 5.53 |
| 12 | .246 | 2.0097 | 0.937 | | 163.83 | / 0.1 |
| 11 | .246 | 2.0147 | 1.222 | | 203.69 | / 5.61 |
| 13 | .246 | 5.0387 | 0.693 | | 128.13 | / 6.18 |
| 17 | .246 | 5.0347 | 1.136 | | 168.5 | / 0.68 |

TABLE 4

TEST DESCRIPTION

| Sample | H approx. inch | Specimen weight between clamps gms | δ inch | Explosive thickness inch | Backing N-Neoprene F-Foam | degrees | Slippage |
|--------|-------------------|---------------------------------------------|------------------|--------------------------------|---------------------------------|---------|----------|
| 6 | .089 | 60.98 | 3.30 | .010 per | F | -0.164 | Necking |
| 4 | .089 | 60.88 | 3.13 | .010 per | F | 0.147 | Necking |
| 5 | .089 | 60.80 | 3.20 | .010 per | F | -0.213 | Necking |
| 2 | .122 | 83.34 | 4.17 | .010 | N and F | 0.246 | Visible |
| 3 | .122 | 83.76 | 3.41 | .015 per | F | 1.015 | Visible |
| 5 | .122 | 83.82 | 6.25 | .015 | N | 0.0 | Necking |
| 10 | .122 | 83.48 | 3.51 | .010 per | F | 0.720 | Visible |
| 20 | .122 | 83.97 | 4.43 | .010 per | F | 0.769 | Necking |
| 21 | .122 | 83.66 | 3.93 | .010 per | F | 0.614 | Necking |
| 19 | .122 | 83.68 | 4.37 | .010 | F | 0.516 | Visible |
| 5 | .189 | 129.28 | 4.44 | .015 | N and F | 1.162 | Minor |
| 10 | .189 | 128.26 | 4.38 | .010 | N | 1.178 | Visible |
| 3 | .189 | 128.09 | 7.78 | .020 | F | 0.392 | Visible |

Table 4 contd.

| Sample | H approx. inch | Specimen weight between clamps gms | δ inch | Explosive thickness inch | Backing N-Neoprene F-Foam | degrees | Slippage |
|--------|-------------------|---------------------------------------------|------------------|--------------------------------|---------------------------------|---------|----------|
| 3 | .246 | 168.44 | 4.30 | .010 | F | 1.260 | Minor |
| 1 | .246 | 168.29 | 5.40 | .015 | F | 1.268 | Visible |
| 6 | .246 | 168.16 | 7.68 | .020 | F | 1.211 | Visible |
| 2 | .246 | 168.20 | 9.40 | .025 | F | .949 | Visible |
| 8 | .246 | 57.04 | 1.36 | .010 | F | .900 | Minor |
| 7 | .246 | 56.63 | 1.82 | .015 | F | 1.129 | Minor |
| 9 | .246 | 57.20 | 2.4 | .020 | F | 1.326 | Visible |
| 10 | .246 | 111.87 | 2.93 | .010 | F | 1.015 | Visible |
| 12 | .246 | 111.57 | 3.95 | .015 | F | 1.277 | Visible |
| 13 | .246 | 280.29 | 7.02 | .010 | F | .900 | Minor |
| 17 | .246 | 280.07 | 9.23 | .015 | F | .974 | Visible |
| 11 | .246 | 111.98 | 4.93 | .020 | F | 1.097 | Visible |

FIGURE 5
W vs X and Y

27

PLATE #19
H 0.1225 m
B ~ 3 m.
2L ~ 5 m.

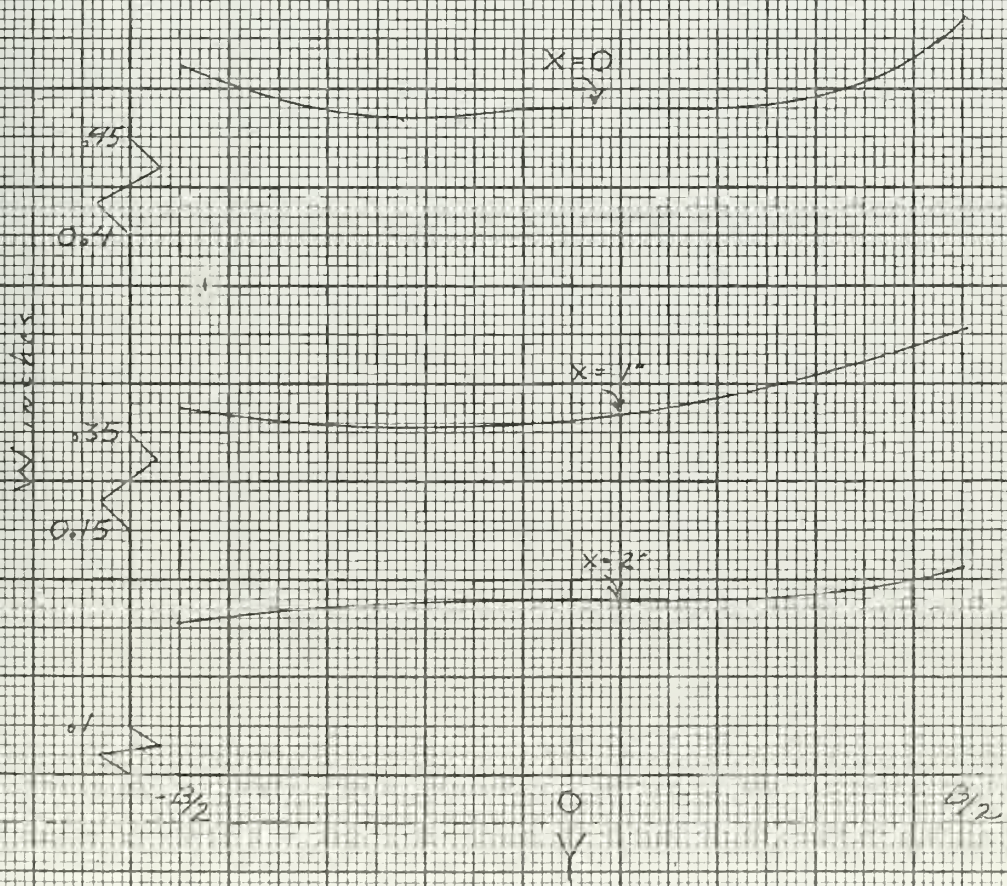
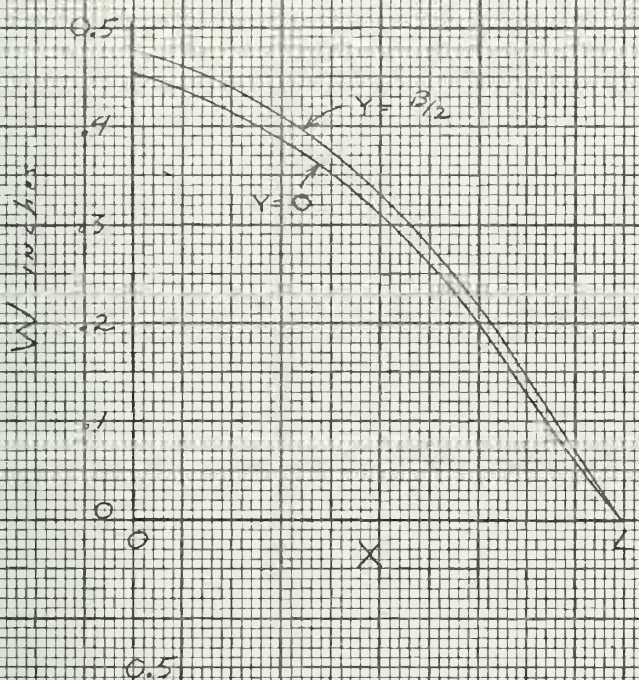


FIGURE 6

2.8

W vs X and Y

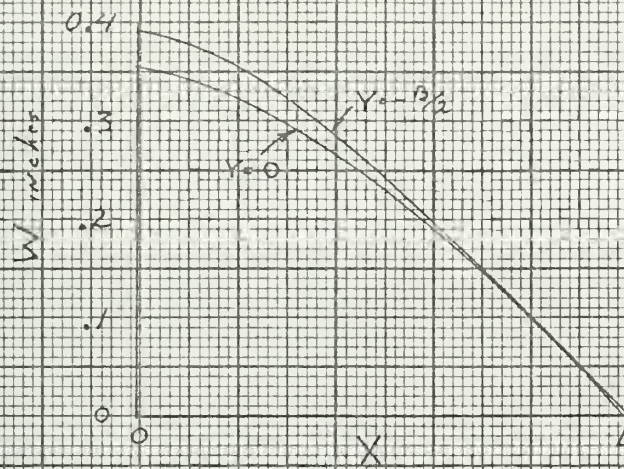


PLATE # 2

| | |
|----|---------------|
| H | 0.189 inch |
| B | ~ 3 inch |
| 2L | ~ 5 inch |

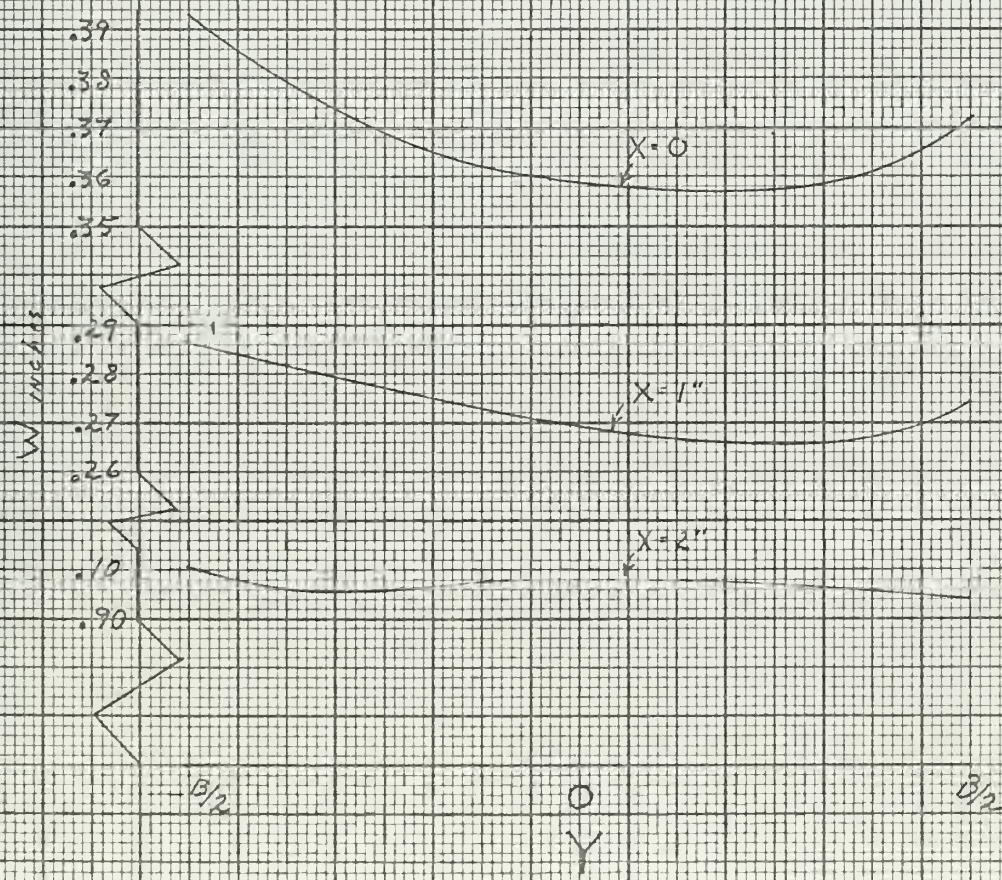


FIGURE 7

29

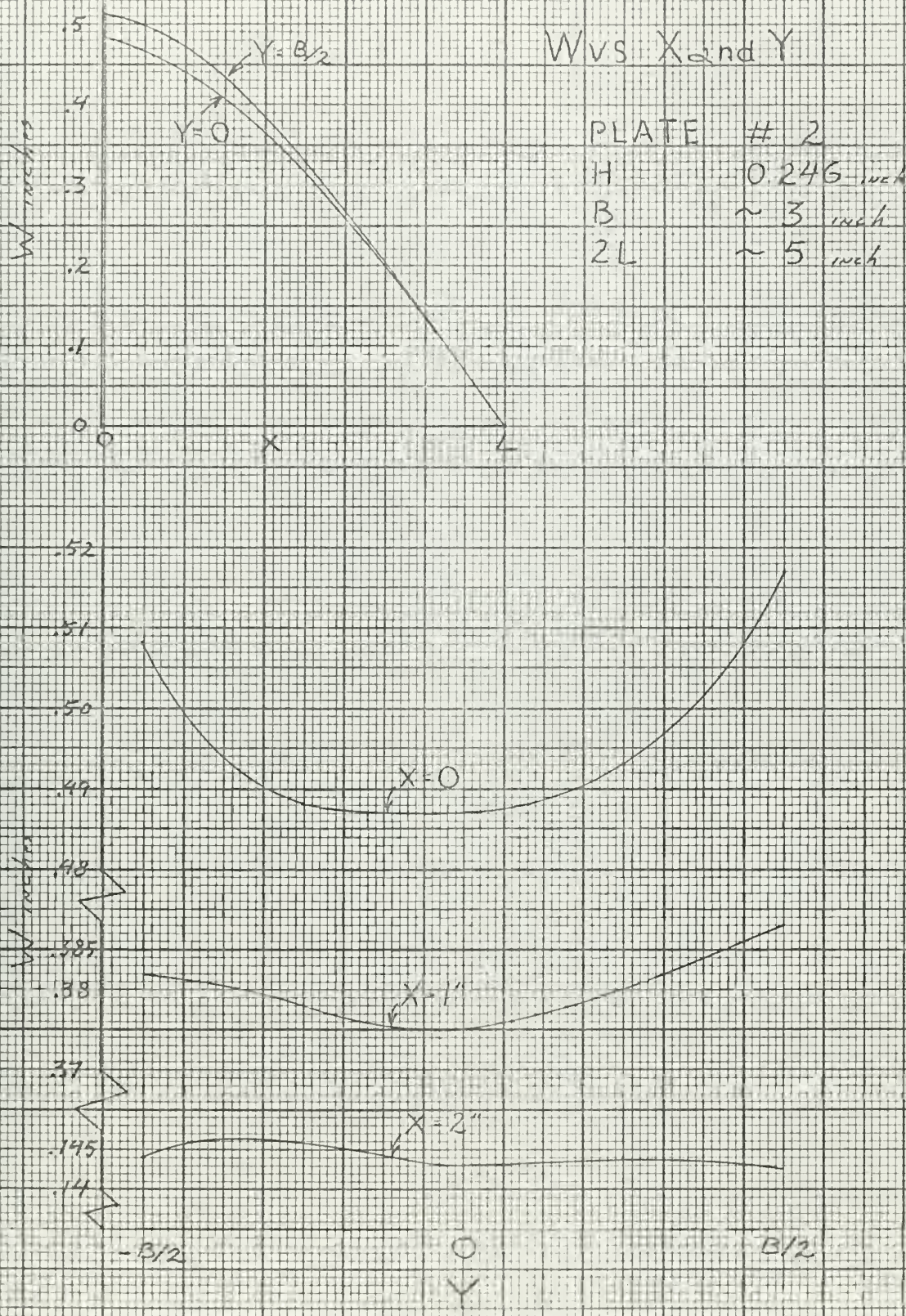


FIGURE 8
Wvs X and Y

30

PLATE #13

H ~ .246 inch

B ~ 5 inch

2L ~ 5 inch

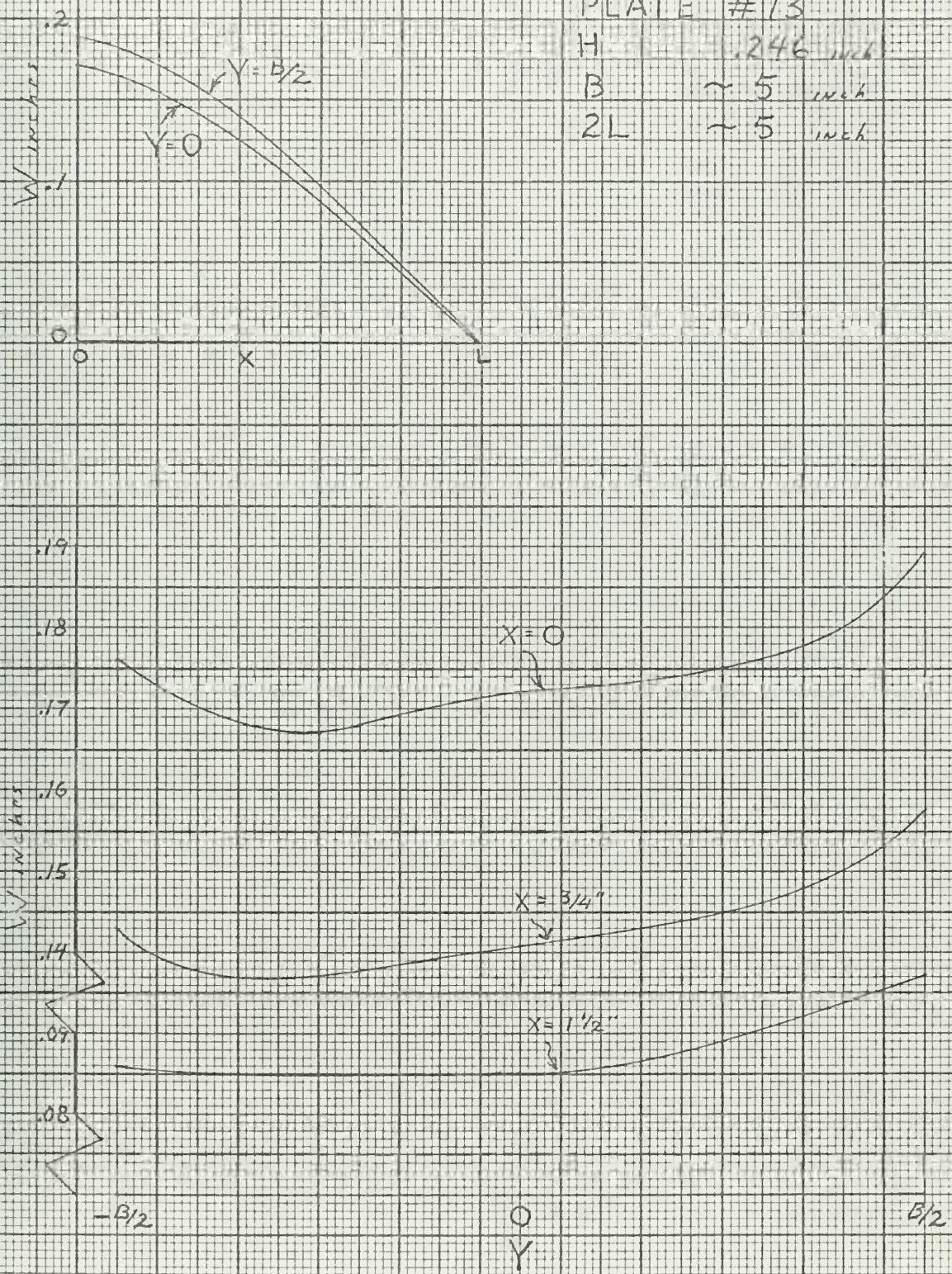


FIGURE 9
W vs X and Y

31

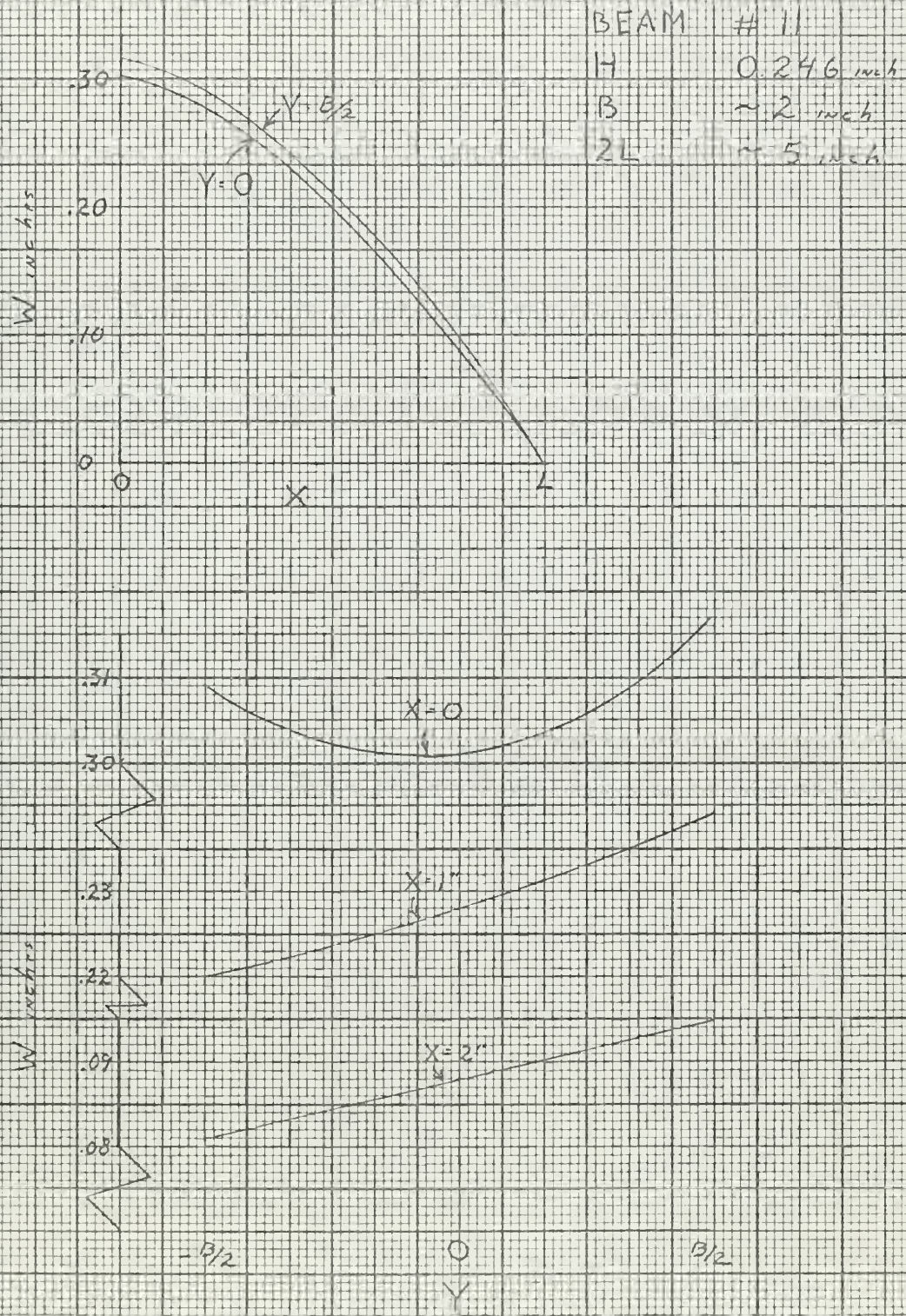


FIGURE 10

32

W vs X and Y

BEAM #7

H 0.246 inch

B ~ 1 inch

2L ~ 5 inch

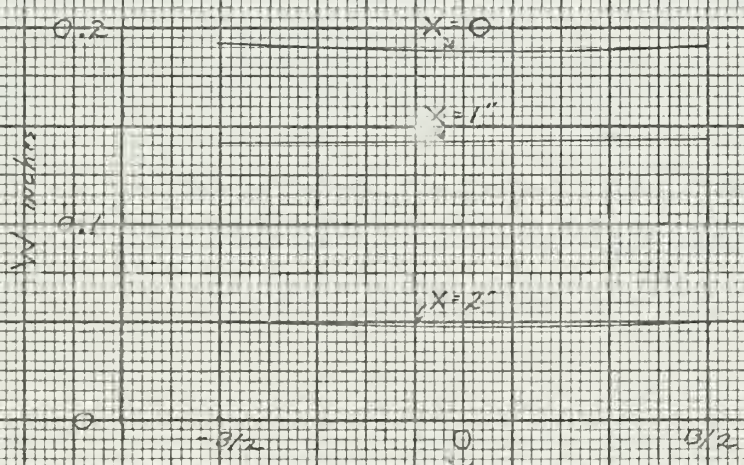
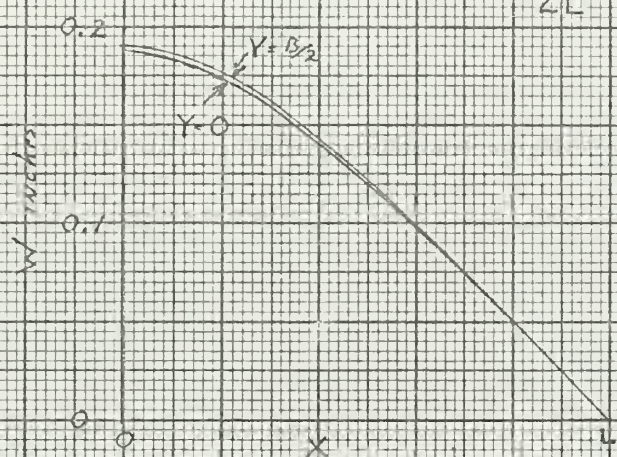


FIGURE II

33

W_m/H and W_o/H vs. V
for $H = 0.122$ inch

$B \sim 3$ inch

$2L \sim 5$ inch

- W_m/H
- △ W_o/H

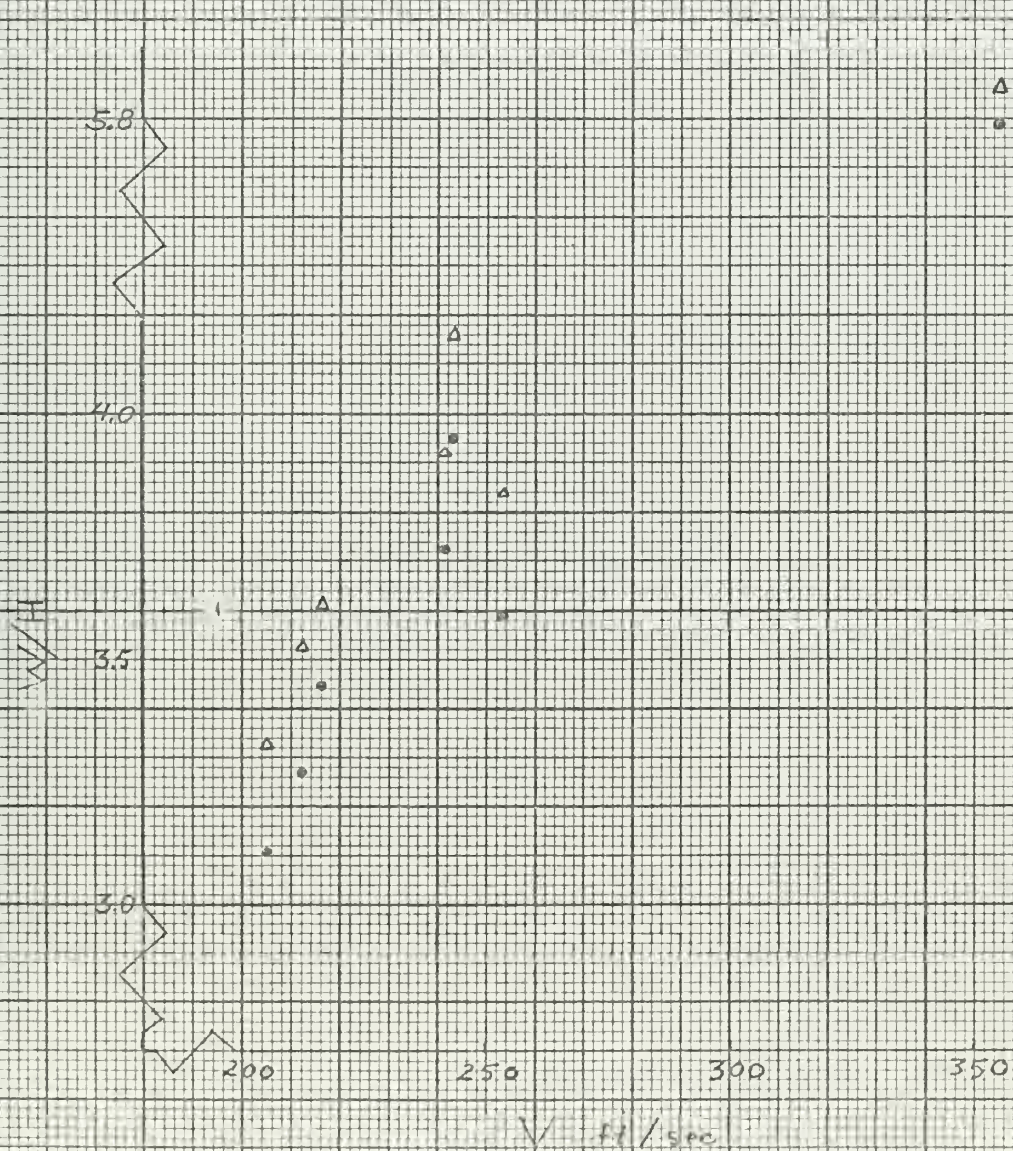


FIGURE 12

34

W_m/H and W_o/H vs. V for $H = 0.189$ inch

$B \approx 3$ inch

$2L \approx 5$ inch

• W_m/H

△ W_o/H



FIGURE 15

 W_m/H vs. V for

$H = 0.246 \text{ inch}$

$2L \sim 5 \text{ inch}$

35

280

250

220

200

180

150

120

90

60

30

0

 ft/sec

A

B

C

D

E

F

G

A

B

C

D

E

F

G

A

B

C

D

E

F

G

A

B

C

D

E

F

G

A

B

C

D

E

F

G

A

B

C

D

E

F

G

A

B

C

D

E

F

G

PLATE $B \sim 3 \text{ inch}$
 PLATE $B \sim 5 \text{ inch}$
 BEAM $B \sim 2 \text{ inch}$
 BEAM $B \sim 1 \text{ inch}$

2.0

1.5

1.0

0.5

0.0

1.00

 H/W_m

FIGURE 14

36

Wn/H vs V

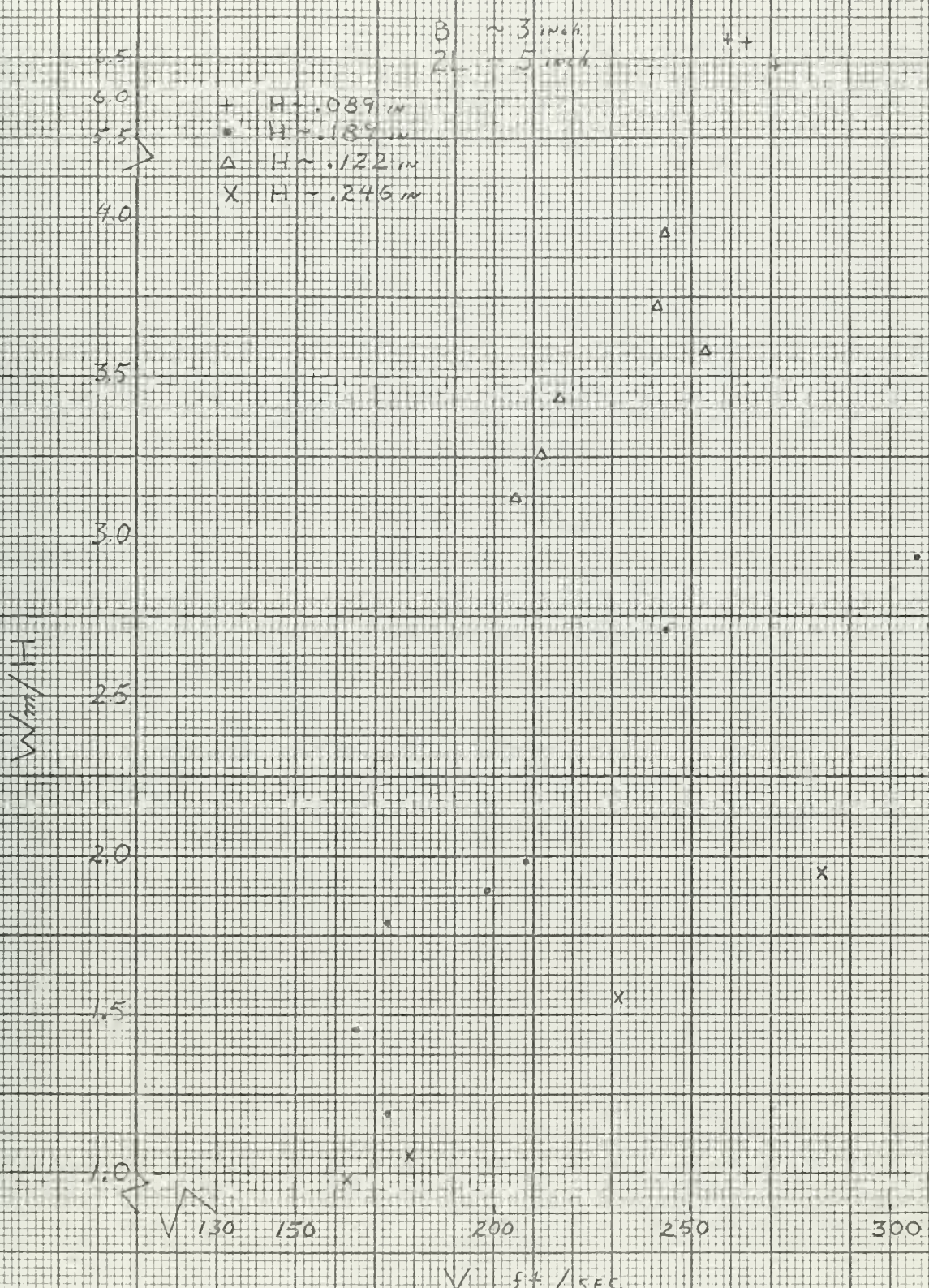
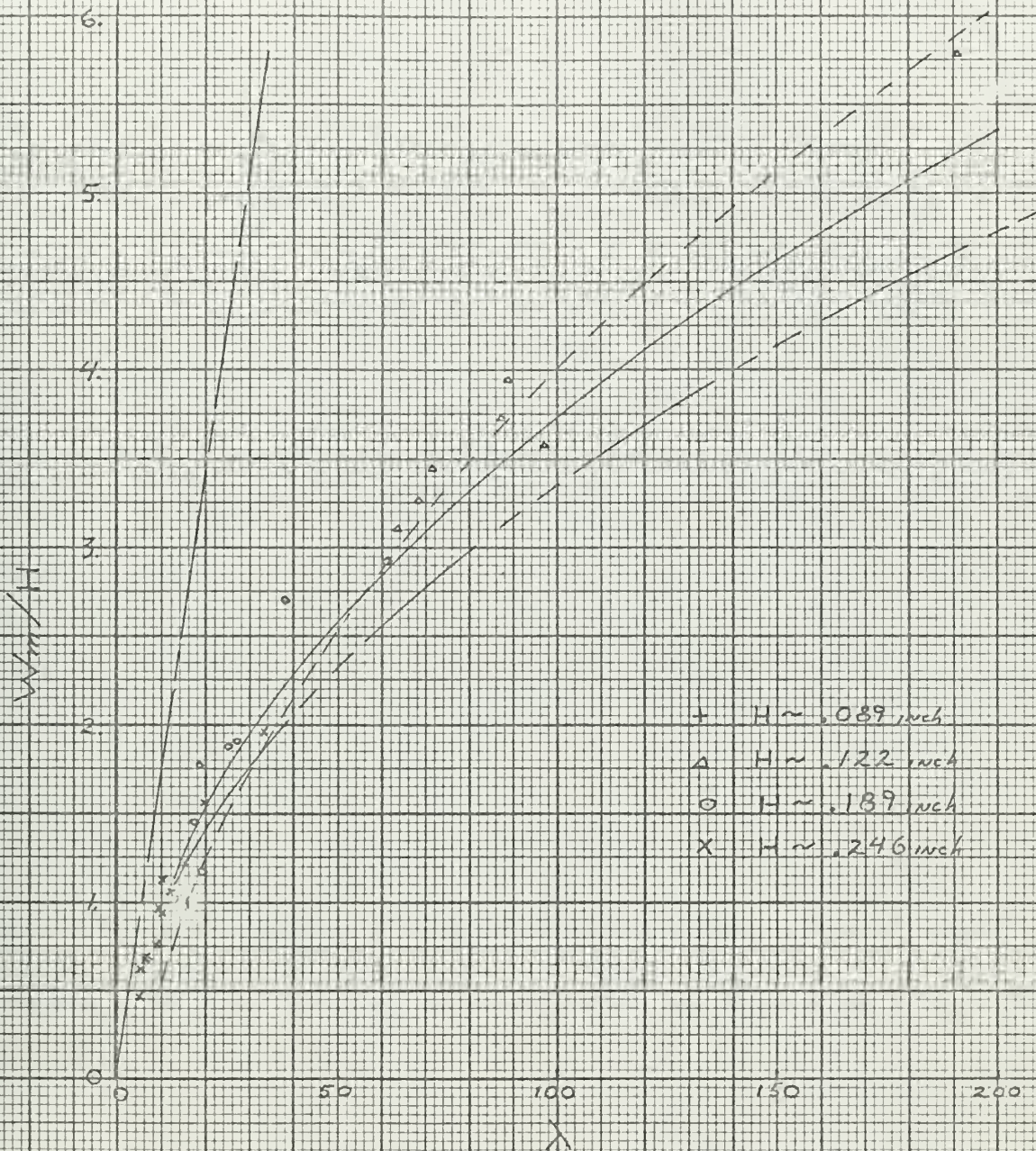


FIGURE 15

37

W_m/H vs λ



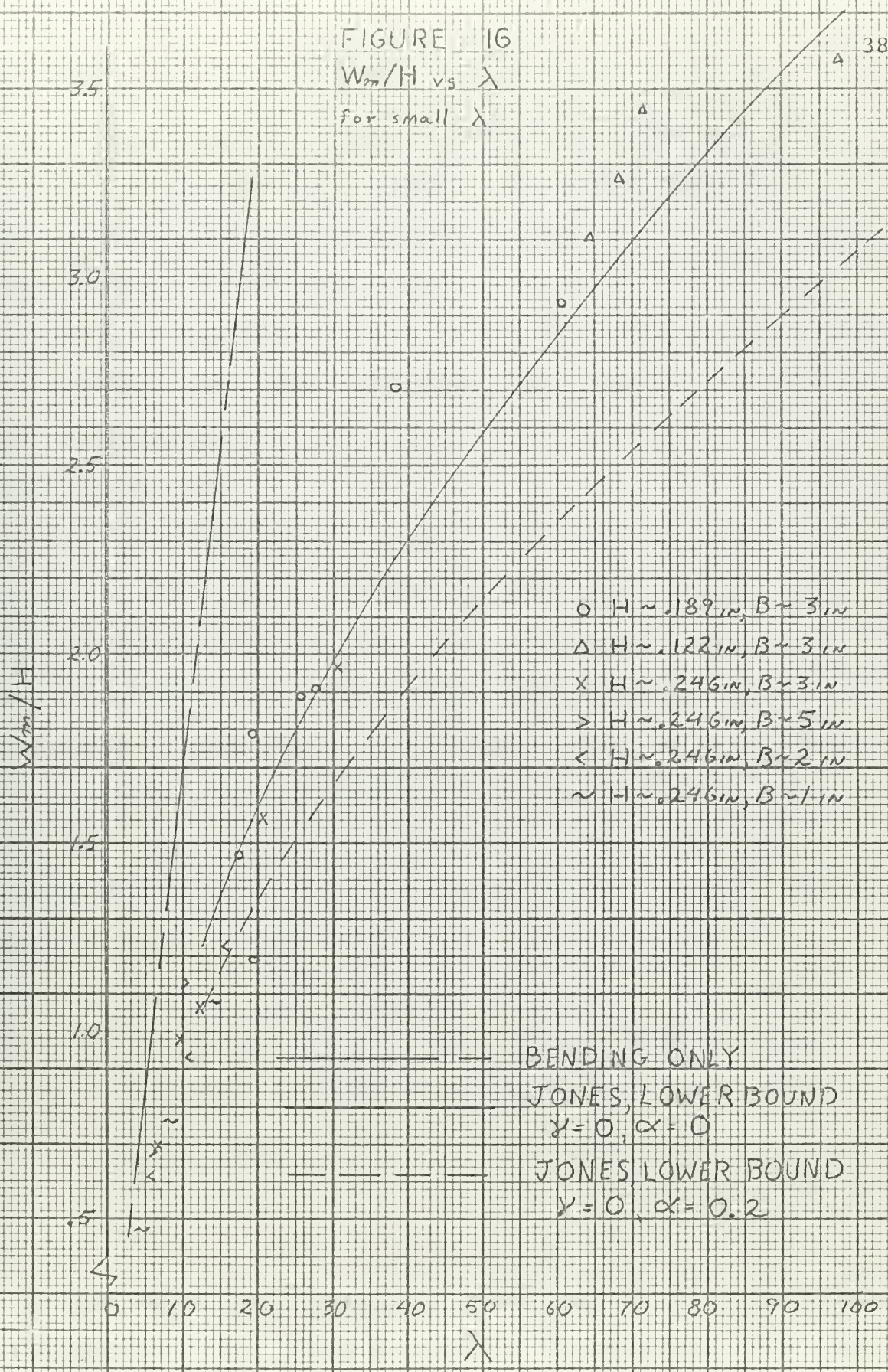
SIMPLE BENDING, CLAMPED ENDS

SYMONDS & MENTEL (5, 13)

JONES, LOWER BOUND (11, 13)

JONES, UPPER BOUND (11, 13)

FIGURE 16

 W_m/H vs λ for small λ 

The tables and figures presented in the previous section display the experimental results for tests on 6061-T6 aluminum plates and beams clamped at two ends which were uniformly loaded by a dynamic impulse. The material is commonly considered rate insensitive and not noted for strain hardening. The low values for α and γ , strain rate and strain hardening parameters, shown in Table 3 verify this assumption.

It is important to recognize that the final permanent deflections recorded W_M and W_O are probably not the maximum deflections that the specimens experienced during deformation. Undoubtedly, some elastic unloading took place. This could be of importance in certain design applications. The deflections were measured after the specimens were removed from the head. The clamped ends of the specimens were found rotated through an angle θ as shown in Figure 4 and tabulated in Table 4. Distinct plastic hinges were observed in all cases at the clamped edge while throughout the center portion of the specimen the plastic region extended over an arc or zone. It is postulated that the type of rotation encountered in all but two of the tests is primarily due to slight elastic unloading of the center portion of the plate or beam. A method was devised to approximately measure the deflection with the specimens clamped in the head. Tests on five

showed that in the worst case $W_M \approx 94\%$. (reported) W_M actual for $\theta = 1.27^\circ$. This seems an upper error limit. As another example, $W_M \approx 99.7\%$ (reported) W_M actual for $\theta = 0.892^\circ$. The check indicated that the error was very slight and no mathematical correction could be found.

The deflection profiles presented in Figures 5 through 10 illustrate that the maximum permanent deflection, W_o , always occurred at the free edges. In the center portion of the specimen, the side away from the impulse was in a state approximating axial tension (between the clamps) while the opposite case existed on the loaded side. This would cause an edge curl through a Poisson effect. In most cases, a transverse cut through the center of the specimen would reveal a cross-section with the edges at about the same deflection, always greater than that at the center line, $x = 0, y = 0$. For certain tests there are marked discrepancies in this, with one edge significantly more deflected than the other, such as in Figure 8 for the 5 inch wide plate. This may signify that a true uniform pressure loading did not exist. When handling sheets of explosive 10 and 15 thousands of an inch in thickness, total homogeneity cannot be expected.

The graphs of W_M/H vs. V show the initial results for the tests. As expected, the thinner plates would deflect more for a given impulse velocity, V . Figure 13 which has the 1 inch, 2 inch, 3 inch, and 5 inch wide beams and plates

all of 0.246 inch thickness and constant length shows no marked transition from beams to plates with two edges clamped. This figure indicates that for a given initial velocity, and constant length, the large the permanent deflection for increasing width, but that to a good first order approximation the plates may be treated as beams.

The parameter $\lambda = \frac{\mu V^2 L^2}{M_0 H}$ was introduced to nondimensionalize the impulse to a common base and cancel out geometry variations.

Figures 15 and 16 appear to plot as a curve and not a group of results. To the author's knowledge, a theory for dynamic loading of the rectangular plates tested has not been established.

The curves of W/H vs. λ exhibit the decreasing slope expected with the dominance of finite deflections, i.e. membrane forces. The results suggest that a simple bending only theory is inadequate for permanent deflections. The bending-only equation plotted, $W_M/H = \lambda/6$, assumes a rigid-plastic material, two stages of motion during deformation, and axial restraints (11). During the first state of motion, hinges are formed at the clamps and progress inward. In the second stage, there is rotation at the clamps and a fixed hinge at the beam center travels to the final deflection. $W_M/H = \lambda/3$ is for the same problem but with simply supported ends.

Significantly, the upper and lower bounds developed by Jones (11, 13) match the results over a large band of possible engineering interest. For these bounds, the rate sensitivity and strain hardening parameters, α and γ , are both equal to zero. This assumes a rate insensitive material. In particular, the "lower bound" correlates quite well with the experimental results through $W_M/H \approx 4.0$. For the largest deformation obtained, the theory is too conservative. Unfortunately, there are not many results for large λ and those achieved must be considered questionable since large slippage occurred. The choice of σ_0 , the yield stress in simple tension, merits consideration. For the 6061-T6 aluminum tested σ_0 was determined by a 0.2% offset method. As an example, if the average yield stress by a 0.4% offset method had been used, $\lambda = 50$ would have been decreased to 49.1. This is a slight alteration.

The plots must be viewed as a representative of the maximum centerline deflection. As discussed before, Poisson effect caused the free edges to reach a larger final deflection.

The expressions "upper and lower bound" are not used in the more commonly understood sense. The upper bound required that the yield surface be everywhere on or outside the exact yield surface, while the lower bound means that the yield surface is everywhere on or inside the exact yield surface. The bounds plotted are a computer solution

for the derivation in reference (11). The solution is for a beam clamped at two ends and assumes the following: rigid-plastic behavior; traveling hinges with two stages of deformation; a linearized yield condition relating the axial bending moment and membrane forces. The reference cited gives a development for pinned ends which may be modified for the clamped end case by introducing plastic

$$\text{hinges, } M_O = \frac{\sigma_0 H^2}{4}, \text{ at the clamped ends.}$$

Figure 15 has a curve which shows the deflections predicted by the theory of Symonds and Mentel (5, 13) for lower bound deformation. For W_M/H greater than about 3 or 3.5, the predictions agree quite well with the experimental results. The derivation was for clamped ends, rigid-plastic behavior, and included finite-deflections. The major difference from that discussed in the preceding paragraph is in the choice of a yield surface. This derivation considered an exact yield surface with necessary approximations, not a linearized yield surface.

Figure 16 has a computer solution plotted which shows the theoretical effect of rate-sensitivity. $\alpha = 0.2$ was chosen as representative of the values of α for the actual test specimens. The strain-hardening parameter is left equal to zero, $\gamma = 0$, for this is representative of the test results. It is evident that introducing the rate

sensitivity gives lower values of W_M/H for a γ than found in the experiments. The plot is based on work in references (11, 13) which introduced rate effects via a constitutive equation proposed by Cowper and Symonds (8)

$$\frac{\sigma}{\sigma_0} = 1 + \left(\frac{\dot{\varepsilon}}{D}\right)^{1/p}$$

CONCLUSIONS

These statements are based on the experimental results of a series of tests in which 6061-T6 aluminum rectangular plates and wide beams, with two edges clamped, were uniformly loaded by a dynamic impulse. It is suggested that the nondimensional plots of the results may be used for plates made of other materials similarly loaded, of negligible rate sensitivity and strain hardening.

There was no significant transition from beam to plate behavior.

Simple bending-only theory over-estimated all permanent deformations greater than half the plate thickness by such a magnitude as to be considered unacceptable.

A beam theory which assumes rigid-plastic behavior, no rate sensitivity, no strain-hardening influences, and which included finite deflections gave good predictions of the experimental deformations for a significant range of impulses.

REFERENCES

- (1) Parkes, E. W., "The Permanent Deformation of a Cantilever Struck Transversely at its Tip," Proceedings of the Royal Society, London, Series A, Vol. 228, 1955, pp. 462-476.
- (2) Seiler, J. A., Cotton, B. A., and Symonds, P. S., "Impulsive Loading of Elastic-Plastic Beams," Journal of Applied Mechanics, Vol. 23, 1956, pp. 515-521.
- (3) Bodner, S. R., and Symonds, P. S., "Experimental and Theoretical Investigation of the Plastic Deformation of Cantilever Beams Subjected to Impulsive Loading," Journal of Applied Mechanics, Vol. 29, 1962, pp. 719-728.
- (4) Ting, T. C. T., "Large Deformation of a Rigid, Ideally Plastic Cantilever Beam," Journal of Applied Mechanics, Vol. 32, 1965, pp. 295-302.
- (5) Symonds, P. S., and Mentel, T. J., "Impulsive Loading of Plastic Beams with Axial Restraints," Journal of Mechanics and Physics of Solids, Vol. 6, 1958, pp. 186-202.
- (6) Humphreys, J. S., "Plastic Deformation of Impulsively Loaded Straight Clamped Beams," Journal of Applied Mechanics, Vol. 32, 1965, pp. 7-10.
- (7) Bodner, S. R., "Behavior of Metals Under Dynamic Loading," edited by N. J. Huffington, ASME, 1965, pp. 93-105.
- (8) Cowper, G. R., Symonds, P. S., "Strain Hardening and Strain-Rate Effects in the Impact Loading of Cantilever Beams," Tech. Report No. 28, O.N.R. Contract Nonr. - 562(10), NR - 064-406, Brown University, 1957.
- (9) Perrone, N., "On a Simplified Method for Solving Impulsively Loaded Structures of Rate Sensitive Materials," Journal of Applied Mechanics, Vol. 32, 1965, pp. 489-492.
- (10) Florence, A. L., and Firth, R. D., "Rigid-Plastic Beams Under Uniformly Distributed Impulses," Journal of Applied Mechanics, Vol. 32, 1965, pp. 481-488.

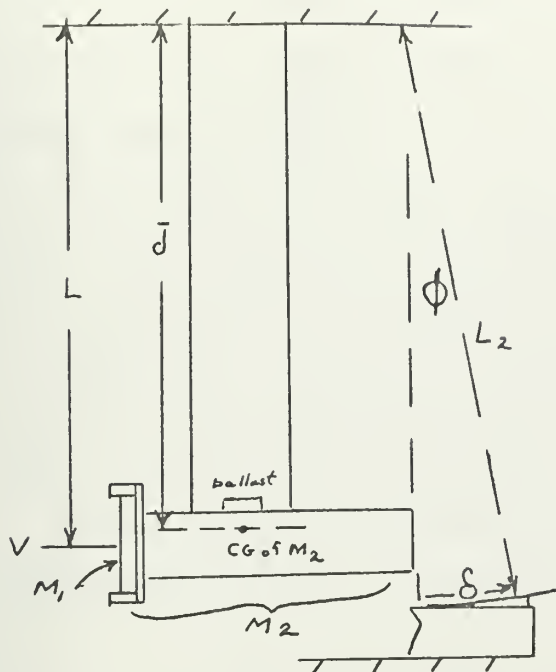
- (11) Jones, N., "Influence of Strain-Hardening and Strain--Rate Sensitivity on the Permanent Deformation of Impulsively Loaded Rigid-Plastic Beams," International Journal of Mechanical Science, Vol. 9, 1967, pp. 777--796.
- (12) Jones, N., "Impulsive Loading of a Simply Supported Circular Rigid Plastic Plate," Journal of Applied Mechanics, Vol. 35, 1968, pp. 59-65.
- (13) Jones, N., "An Experimental Study Into the Behavior of Beams Subjected to Large Dynamic Loads," to be published by the Department of Naval Architecture and Marine Engineering, M. I. T.
- (14) Florence, A. L., "Traveling Force on a Timoshenko Beam," Journal of Applied Mechanics, Vol. 32, 1965, pp. 351-358.
- (15) Griffin, R. N., "Finite Deflections of Impulsively Loaded, Rigid Rectangular Mild Steel Plates with Two Edges Clamped," Naval Engineer's Thesis, Department of Naval Architecture and Marine Engineering, M. I. T., June, 1969.
- (16) Goldsmith, W., "Impact," Edward Arnold Publishers, Ltd., London, 1960.
- (17) Uran, Tevfik O., "A Study Into the Damage to Rectangular Plates Subjected to Dynamic Loads," Master of Science Thesis, Department of Naval Architecture and Marine Engineering, M. I. T., June, 1969.

APPENDIX A

Experimental Recommendation

Achievement of a rigidly clamped edge is extremely difficult and some slippage experienced in this work casts doubt on the results for λ much greater than 200. Professionally toothed gripping heads and high strength bolts are a definite requirement. It is suggested that further improvement may be obtained by machining specimens for which the ends to be clamped are much thicker than the test portions between the clamps used in reference (13) on beams.

APPENDIX B

Calculation of V

M_1 = mass of the target between the clamps

M_2 = mass of the entire system including M_1

\bar{d} = distance to center of gravity of M_2

$$I_1 = M_1 L^2$$

$$I_2 = M_2 \bar{d}^2$$

w = angular velocity of notation

To account for the shift in the center of gravity as various ballast weights were added, a derivation from reference (1) was used which is briefly shown

$$I_2 w = LM_1 (V - LW) \text{ or } V = \frac{w I_2 + M_1 L^2}{M_1 L}$$

$$\frac{1}{2} [I_2 + M_1 L^2] w^2 = g(M_1 + M_2) \bar{d} (1 - \cos \phi)$$

$$V = \frac{2g(I_2 + I_1) \bar{d} (1 - \cos \phi) (M_1 + M_2)}{M_1 L}$$

$$\phi = \delta/L_2$$

The weights of all components were known. For each test, the weight of ballast and the weight of the entire test plate including the portion between clamps was recorded. The height of the pendulum from the floor was recorded since the height from the floor to suspension system was known. During the test δ was measured by means of a hot wire. The weights of all components were used to determine the location of the center of gravity of M_2 , hence \bar{d} .

The exact dimensions of the sample between the clamps and its mass density was used to determine M_1 .

For a simplified example, as \bar{d} approaches L , i.e. disregard the shift in the center of gravity.

$$V = \frac{(M_1 + M_2)}{M_1} \quad 2gL (1 - \cos \phi)$$

Consider plate number five

$$H = 0.246 \text{ in.}$$

$$2L = 5.046 \text{ in.}$$

$$B = 3.025 \text{ in.}$$

Added ballast for stabilization = 3653 gms.

$$\delta = 6.49 \text{ in.}, L_2 = 133.425$$

Distance from floor to base of I beam = 7.75 in.

$$M_2 = 29431 + 3653 + 285 = 33369 \text{ gms}$$

$$M_1 = (44.82) (5.046) (3.025) (.246) = 168.5 \text{ gms}$$

$$\phi = \frac{6.49}{133.425} (57.296) = 2.76^\circ$$

$$\begin{aligned} L &= 138.8 - (\text{half depth of pendulum and height} \\ &\quad \text{from floor to bottom of pendulum}) \\ &= 138.8 - (2.4875 + 7.75) = 128.5 \end{aligned}$$

thus

$$\begin{aligned} v &= \frac{(33537.5)}{168.5} \quad 2g(128.5) (1 - \cos 2.76) \\ &= 199.99400 (.00095) = 1985 \text{ in./sec} = 166 \text{ ft./sec.} \end{aligned}$$

The actual value using the full equation and not rounding off significant figures is 179.16 ft./sec. A computer program was used to ensure three place accuracy.

APPENDIX C

Tensile Test Results

All tensile test specimens were of a straight parallel side configuration as allowed by ASTM standards for sheet specimens. Tests were made in tension on an Instron testing machine with a Baldwin microformer instrrometer for strain indications. The specimens were nine inches in length and the instrrometer had a one inch gage length. Calculations are based on original cross section areas. The yield stress, σ_0 , is by the 0.2% offset method.

| | | | | | | | | |
|------------------------------------------|-------|-------|--------|-------|-------|------------------------------------|-------|-------|
| Sample | 16 | 7 | 9 | 8 | 4 | 6 | 19 | 18 |
| Width (in) | .508 | .505 | .504 | .507 | .503 | .492 | .508 | .509 |
| Thickness (in) | .089 | .1225 | .1225 | .1225 | .187 | .189 | .246 | .246 |
| Cross section Area (in ²) | .0452 | .0619 | .06175 | .0621 | .0941 | .0929 | .1249 | .1252 |
| Instron Head Speed (in/min) | .05 | .05 | .1 | 1 | .05 | 1 | .05 | .05 |
| Yield Load (lb) | 1890 | 2500 | 2590 | 3770 | 3850 | 5180 | 5180 | 5180 |
| σ_o (psi) | 41800 | 41300 | 40500 | 41700 | 40100 | 41400 | 41500 | 41400 |
| $E \times 10^{-6}$ (psi) | 9.85 | 10.5 | 10.85 | 11.68 | 10.75 | 9.78 | 10.8 | 9.4 |
| Ult Load (lb) | 2860 | 2800 | 2860 | 4340 | 4150 | | | |
| σ_{ULT} (psi) | 46200 | 45300 | 46000 | 46100 | 44700 | | | |
| | | | | | | σ_o avg 2% offset 41212 psi | | |
| | | | | | | $E \times 10^{-6}$ avg 10.49 psi | | |
| | | | | | | σ_{ULT} avg 45660 psi | | |

For comparative purposes these results are shown for the yield stress by the 0.15% offset and 0.40% offset methods.

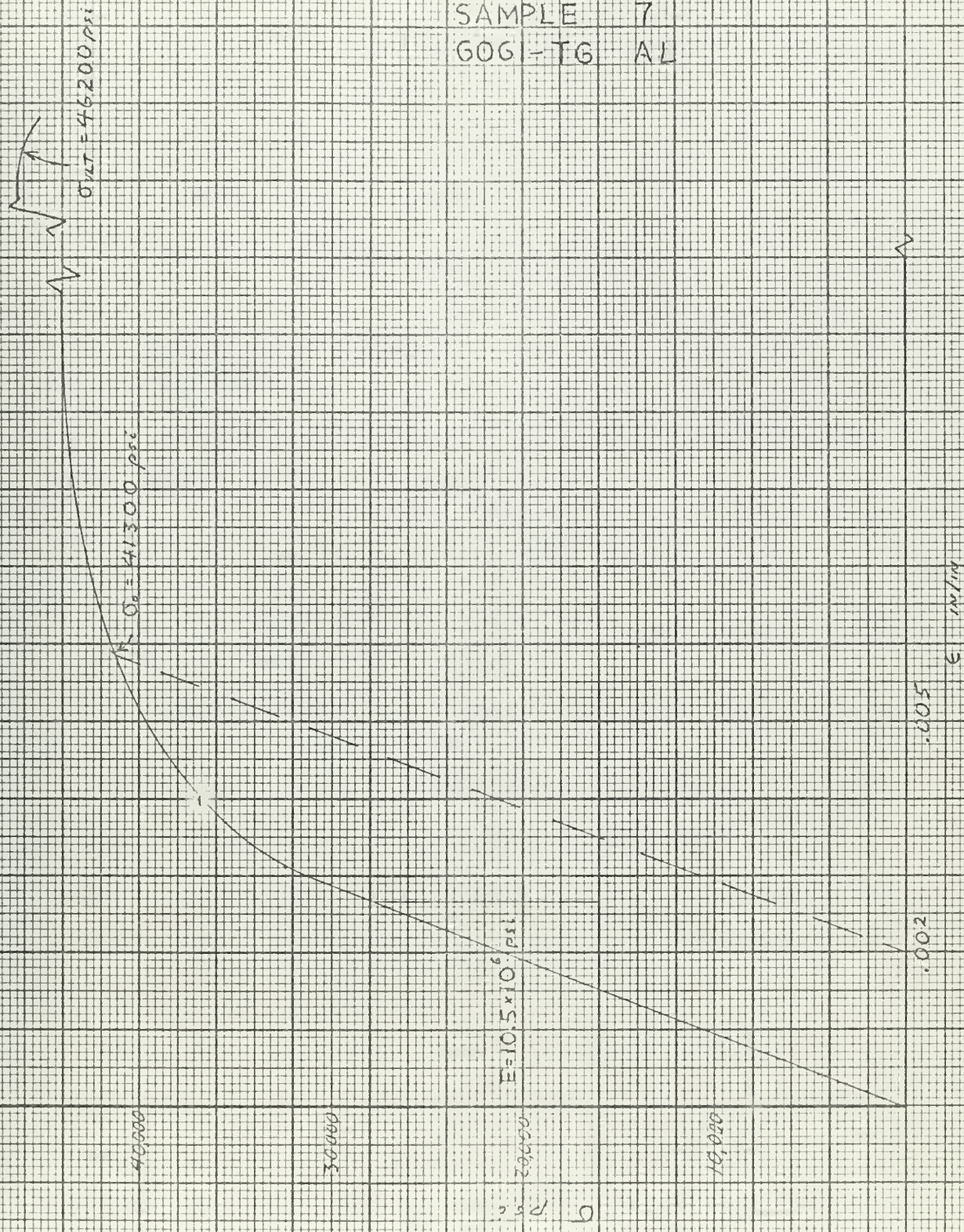
| Sample | 16 | 7 | 9 | 8 | 4 | 6 | 19 | 18 |
|-------------------------------|-------|-------|-------|-------|-------|-------|-------|-------|
| σ Yield psi by .15% offset | 41800 | 41000 | 39900 | 41200 | 39700 | 41300 | 40800 | 40700 |
| σ Yield psi by .4% offset | 41800 | 42600 | 41750 | 42700 | 41200 | 42000 | 42100 | 42000 |

σ Yield avg. by 0.15% offset = 40800 psi

σ Yield avg. by 0.4% offset = 42019 psi

FIGURE 17

56

STRESS vs STRAIN
SAMPLE 7
GOG-TG AL

APPENDIX D

Strain Gage Results

Figure 18 shows the oscilloscope photograph with scales added for a gaged specimen.

Pertinent data is:

Aluminum 6061-T6 beam No. 9

Dimension of beam 0.246 in. thick
1 inch wide
5 inches in length

Impulsively loaded by a .020 inch sheet of
Datasheet D

V, Impulse velocity = 193.6 fps.; $\lambda = 14.1$

Gage: Baldwin-Lima-Hamilton
SR4 type PA-3 Lot 232-11
Gage Factor = $1.95 \pm 1\%$
Gage Resistance = 121 ± 1 ohms
Grid Length = $3/4$ inch
Grid Width = $27/64$ inch
Mounted with SR-4 Post Yield Cement (a nitro-cellulose cement)

The gage is a post-yield type gage supposedly good up to 9-10% strain.

A balanced bridge was used with a single active gage.

The strain indication was a Dumont Strain Gage Control, type 335. Oscilloscope settings were 50 microseconds per centimeter time sweep and 20 milivolt per centimeter for deflection.

The scope and camera were initially triggered by a wire placed over the explosive leader from the detonator to the explosive on the sample. The response was apparently instantaneous for no time interval was marked

before the gage responded. Unfortunately, the initial strain rate was not marked. This is not explained by a single result. Obviously, a faster time sweep may be required.

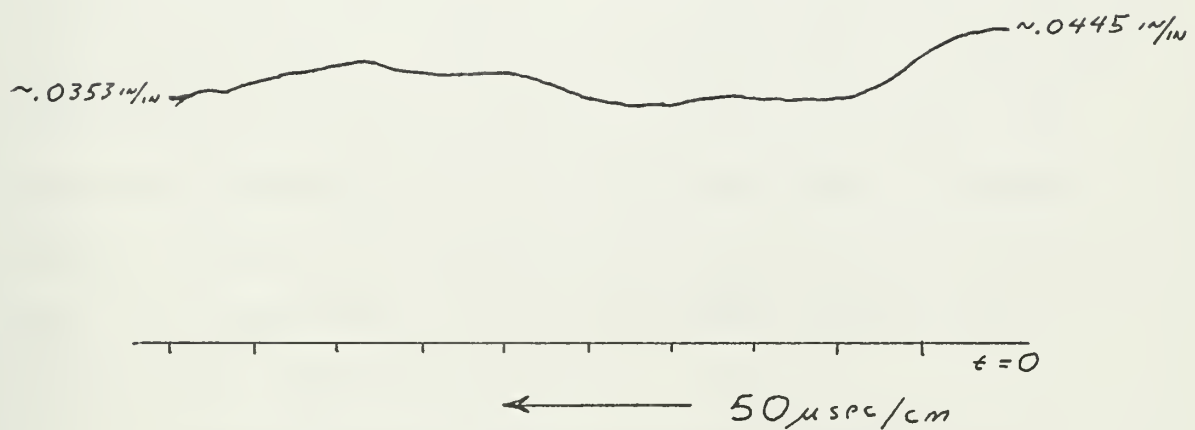
The maximum strain was reached on the initial plate deflection and is on the order of 4.45% strain. Afterwards, the beam appears to have entered an oscillatory phase and perhaps experienced a final strain on the order of 3.5%. These figures must be taken as average strain over a region since the gage grid length was 3/4 of an inch.

Two additional SR4 Type PA-3 gages failed in use. In both cases, the failure occurred at the juncture of the external leads. The gages failed so suddenly that an initial strain rate was not obtained. The leads were placed in such a manner as to allow some slack. Even so, the initial inertial force upon the leads and gage was enough to rip the gage connecting leads from the carrier.

Tests with a small Budd metal film Type HE-11, Lot A25-KJJ-1 gage was wholly unsatisfactory. This type gage is on the order of 1/8 inch grid length. Such a small size gage cannot remain in place under the high initial loads exerted by its own leads and the external lead wire.

FIGURE 18

STRAIN vs TIME
for BEAM # 9



APPENDIX E

Datasheet Specifications

The explosive used for this series of test was Datasheet D manufactured by E. I. DuPont. It is a flexible sheet explosive composed of PETN (Pentaerythritol Tetranitrate) and an elastomeric binder. Sheets of .010 inch and .015 inch in thickness were purchased. The explosive is easy to handle, has a high detonation velocity, and is safe to use. Safety in explosive work, it must be emphasized, is a function of the product and user. For the tests conducted, full advantage was taken of expert advice offered by the manufacturer, State Safety Office, local Fire Department, University Safety Office, and a private user, AVCO Corporation.

A blasting chamber designed for one pound of TNT was available for actual testing.

The manufacture recommends specific electric detonators for use with Datasheet. It was found that a No. 6 electric detonator provided completely reliable service when aligned with its nose directed into a small patch of Datasheet at least .03 inch thick and backed by a steel plate. This patch ignited the leader which was 1/8 inch wide and 0.015 inch thick.

Datasheet Properties

| | |
|---------------------------------|--------------------------------------|
| Explosive Content | 63% PETN |
| Detonation Velocity | 7000 meters/sec |
| Density | 1.48 gms/sec |
| Flexibility Range | -65 to 160° F |
| Thermal Stability °F | |
| 24 hours | 250 |
| 1 hour | 275 |
| Hot bar Ignition Temperature °F | |
| Instantaneous | 565 |
| 30 seconds | 353 |
| Impulse Constant | 20×10^4 dyn - sec per gm |

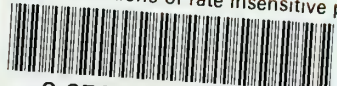
Electric Detonators

Number E-1A6

| | |
|------------------------------|-------------|
| Base Charge | 4.9 gm PETN |
| Resistance | 1.10 ohms |
| All fire current | 0.5 amp |
| No fire current | 0.1 amp |
| Average firing time @ 5 amps | 4 mili-sec |



thesV163
Finite deflections of rate insensitive p



3 2768 001 89000 7
DUDLEY KNOX LIBRARY